JOURNAL OF SPACECRAFT AND ROCKETS
Vol. 41, No. 1, January–February 2004

Applications of Uncertainty Analysis to Architecture Selection of Satellite Systems

Myles A. Walton* and Daniel E. Hastings†
Massachusetts Institute of Technology, Cambridge, Massachusetts 02139

One of the most significant challenges in conceptual design is managing the tradespace of potential architectures: choosing which design to pursue aggressively, which to keep on the table, and which to leave behind. The application is presented of a framework for managing a tradespace of architectures not through traditional effectiveness measures such as cost and performance, but instead through a quantitative analysis of the embedded uncertainty in each potential space system architecture. Cost and performance in this approach remain central themes in decision making, but uncertainty serves as the focal lens to identify potentially powerful combinations of architectures to explore concurrently in further design phases.

Nomenclature

k	=	risk aversion coefficient
Q	=	covariance matrix
Q_D	=	downside scaled semivariance covariance matrix
r	=	return of an architecture, units vary with mission
S_D	=	scaled semivariance, units vary with mission
$U_{\text{h\_surv}}$	=	utility of high-latitude survey mission
$U_{\text{l\_snap}}$	=	utility of low-latitude snapshot mission
$U_{\text{l\_surv}}$	=	utility of low-latitude survey mission
U_T	=	total utility
w	=	investment weightings for architectures considered
ρ	=	correlation
σ	=	standard deviation, units vary with mission
$\sigma x, y$	=	covariance, units vary with mission

Introduction

CONSISTENT with the complexities of a space system, conceptual design is plagued with uncertainties from sources both identifiable and concealed. It is the job of those involved to wade through the uncertainty that defines the problem and select architectures that, within the current level of available information, reflect the better alternative. It is clear that, in uncertain environments, optimality is something of a myth. However, the simplistic assumptions of certainty of conditions, even at the embryonic stages of design, can yield detrimental conclusions. This paper lays the framework for a new way of looking at the process of exploring potential space system architectures through the lens of uncertainty that has the potential to change the way people think about early conceptual design and the selection of designs to pursue.

Decision criteria such as cost, performance, and schedule are the standard when it comes to decision making in space systems design. These measures, quantified using anything from back of the envelope estimation to expert opinion to intense computation and modeling, serve as the basis of the information provided to the decision maker. The mechanism to calculate information, such as cost, schedule, and performance, has been discussed in a number of books on the design of space systems in addition to the industrial practice exercised at each contractor and continues to be the subject of a large body of research. In contrast, methods of accounting for uncertainty in predictions in space systems design have been far less published. No method has been presented that aggregates the types and sources of uncertainty that are typical of a space system and demonstrates an approach to manage such information. This paper presents such an approach and goes further to develop a framework in which to explore the implications of uncertainty in different architectures.

Figure 1 shows a conceptual design flow with the inclusion of the proposed uncertainty analysis framework. Lying between concept generation and concept selection, the uncertainty analysis approach provides information to the decision maker in preparation for selecting architectures to pursue. The uncertainty analysis location, as described, would be early enough in conceptual design to positively influence decisions, while at the same time late enough so that the problem boundaries are drawn and sources of uncertainty can be identified, assessed, and quantified.

There are three cases investigated in the application of the uncertainty framework: a space-based radar space system, a space-based broadband communications systems, and a space-based ionospheric mapping mission. These three cases represent the three overarching segments of space systems, namely, military, commercial, and civil (science) missions. Each case demonstrates the applicability of the uncertainty analysis approach to the broad class of missions that each represents

The first section in each case describes the overall mission, as well as the conceptual design model description. All cases were modeled using the generalized information network analysis (GINA) method, as described by Shaw et al.[1] In the next section, the focus is on quantifying the architectural uncertainty embedded in each architecture, whereas in the third section, the application of portfolio theory to the individual case is described. Finally each case is closed with insights and conclusions.

Technology Satellite Mission and Model Description

The Technology Satellite of the 21st Century (TechSat 21) program is aimed at pushing the boundaries of current satellite systems development. The most striking feature of the TechSat 21 architecture is the departure from the traditional monolithic satellite designs of the Milstar and defense support program satellites toward collaborative clusters of satellites in what is hoped to be a more flexible, extensible, better performing, and less costly architecture. When a cluster of formation-flying satellites is used, a synthetic aperture can be created for a variety of missions ranging from space-based radar to ground moving-target indication. The case provides a good example of the uncertainty analysis approach applied to a highly complex, high-technology, and envelope-pushing problem.

Received 16 January 2003; revision received 27 May 2003; accepted for publication 12 June 2003.

*Research Assistant, Department of Aeronautics and Astronautics; currently Associate, Morgan Stanley, New York, NY 10036. Member AIAA.

†Professor, Department of Aeronautics and Astronautics, 77 Massachusetts Avenue, Building 41-205. Fellow AIAA.

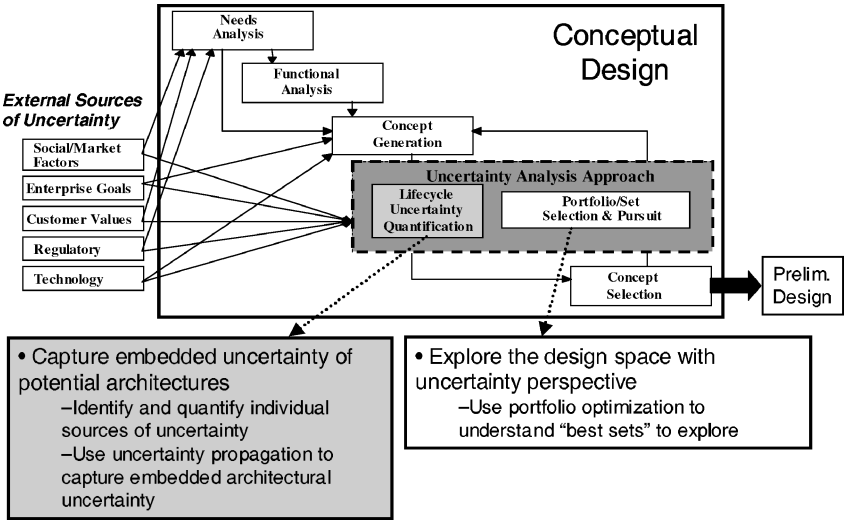

Fig. 1 Insertion of the uncertainty analysis approach in conceptual design.

To conduct a systems analysis of the potential architectures that could be employed to accomplish the TechSat 21 mission, boundaries were established as to what concepts would be evaluated. The different architectural characteristics considered were 1) altitude, 2) number of satellites, 3) number of clusters, 4) number of planes, 5) antenna power, and 6) antenna diameter. In the GINA terminology, these characteristics are called the design vector and a combination of the six design variables constitutes a separate architecture.

GINA Model

The TechSat 21 GINA model developed in the MIT Space Systems Laboratory was essential to completing this case study.[2] The broad architectural concept for TechSat 21 consists of a set of collaborative, formation-flying spacecraft in low Earth orbit that perform multiple missions ranging from synthetic aperture radar to ground moving-target indication to signal interception. The initial modules of the simulation are the design vector, as already described, and the constants vector, representing those variables that for the enumeration of the tradespace are held constant.

Once the design vector and the constants vector have been initialized, the simulation proceeds with the constellation module, which produces the orbital characteristics for the space segment that make it possible to assess the performance of the architecture. The radar module then quantifies the various technical performance measures including probability of detection, minimum detectable velocity of a ground target, and area search rate. The payload sizing module uses the inputs of the design and constants vector to model an appropriate payload antenna for a given architecture, which then prompts the satellite bus module to design an appropriate configuration and size all subsystems to satisfy the payload requirements in terms of power and mass. Once the satellites and their payloads have been modeled, the launch sequence is determined by the launch module, whereas the operations module defines the operational requirements for the system in terms of people, ground stations, etc. The final module, the systems module, using outputs from the preceding model as inputs, generates outcome measures for each architecture, such as total life-cycle cost as well as cost per function measures.[2,3]

Model Results

The GINA model was evaluated for thousands of potential architectures, and various outcome measures were generated to provide input to decision makers. Although all outcome measures are of interest, the primary performance decision criteria chosen was probability of detection, whereas the primary cost decision criteria is life-cycle cost.

With knowledge of the primary decision criteria as probability of detection and life-cycle cost, the Pareto optimal front was found

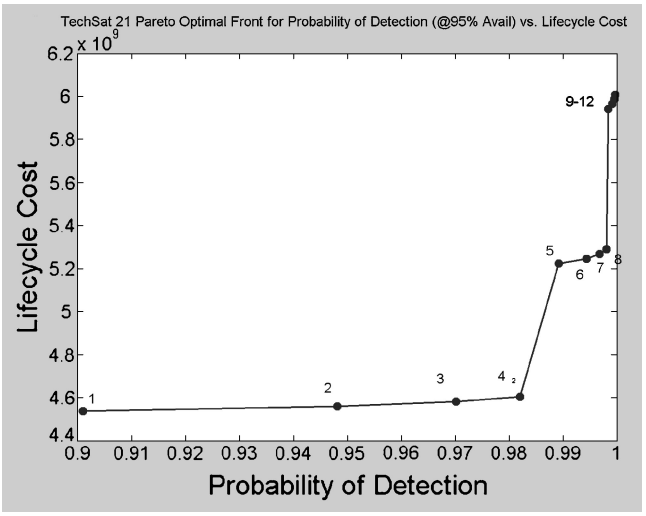

Fig. 2 Pareto optimal front for TechSat 21 architectures.

for the tradespace by identifying nondominated architectures. A nondominated architecture is one whose performance cannot be surpassed without higher costs. Figure 2 shows the Pareto optimal front, as calculated by Jilla using heuristic search methods.[2]

The results just presented were achieved deterministic assumptions and calculations, but by applying the uncertainty analysis approach, it is shown that there is a considerable amount of uncertainty associated with each architecture, that the uncertainty can be quantified, and that portfolio theory provides a central framework in which the uncertainty of the tradespace can be managed.

Uncertainty Quantification

The first step in quantifying embedded architectural uncertainty is to target the sources of uncertainty appropriately. There are two primary reasons not to include all sources of uncertainty in practice. The first is that the analysis would quickly become intractable, and the second reason is that there are some sources of uncertainty whose effects would be either very difficult to model or have little impact on the architectural uncertainties. The uncertainty categorization developed is presented in Table 1. This classification helps to both encompass the various types of uncertainty and guide designers probing for potential uncertainties, as well as to serve as a framework for dialog.

Once the sources are identified, each source is assessed for inclusion in the analysis and, if included, quantified. After the

identification, assessment, and quantification of individual sources of uncertainty, the same GINA simulation models developed earlier are used to quantify embedded architectural uncertainty through uncertainty propagation. These uncertainties were chosen from the constants vector and represent both technical uncertainty, that is, achievable false alarm rate, and model uncertainty, that is, tram cost density for the TechSat 21 mission.

After the individual sources of uncertainty have been identified and quantified, the next step is to develop distributions of outcomes for each architecture. In this case, the extreme method of uncertainty propagation was used in which a single state, best, worst, or expected, is selected and incorporated into the constants vector. This process of selecting a constants vector is repeated until outcome measures have been generated for all states. This uncertainty quantification can be done for each of the architectures in the tradespace or, as suggested here, an efficient tradespace preprocessor can be used to develop a substantially smaller set of architectures from which to conduct uncertainty analysis.

Portfolio Analysis

Knowing the architectural uncertainty can help decision makers in a number of circumstances, such as developing a mitigation plan once an architecture has been selected. When the portfolio optimization of Eq. (1) is used, the decision maker can create tradeoffs and begin to manage the uncertainty in not just an individual architecture, but also the uncertainty in a tradespace of potential architectures:

$$\text{maximize} \quad r^T w - \frac{k}{2} w^T Q w, \qquad \text{subject to} \quad \sum_{i=1}^{n} w_i = 1$$

$$\text{subject to} \quad w \geq 0 \tag{1}$$

In all, only 3 of the original 12 Pareto optimal architectures contribute to portfolios along the efficient frontier. Furthermore, the frontier does not extend beyond any individual architectures in the tradespace and instead represents a linear combination of only three assets. The reason for this limited membership is the high degree of correlation that the architectures being considered share, that is, all $\rho_i \geq 0.998$.

Quantifying Decision Maker Risk Aversion

Once the efficient frontier has been calculated, the next step is to determine where the optimal strategy is for a given decision maker by understanding the risk aversion, which can be straightforward through the use of indifference curves and isoutility lines. Rather than chose a single decision maker's aversion, two decision makers, who represent extremes, as well as a more moderate decision maker are used in the portfolio analysis: risk aversion coefficient k values of 0.5, 2, and 3.

The isoutility lines for the high-risk averse decision maker, $k = 3$, are overlaid on the efficient frontier in Fig. 3 showing the his optimum portfolio at the tangent point of the efficient frontier and the maximum utility isoutility line. The portfolio consists of a single architecture, as do the other decision makers (Table 2).

Implications of Incorporating the Extensions to Portfolio Theory

The impact of separating the upside and downside of uncertainty is explored within a reapplication of portfolio optimization. The first step is to differentiate the risk from the uncertainty in the distribution. The risk can be found by focusing on the downside semivariance. To do so, first adjust the variance of individual observations around the expectation as shown in Eq. (2). Then, calculate the variance of these new observation errors, as shown in Eq. (3). Thus,

$$[r_i - E(r)]^- = \begin{cases} [r_i - E(r)], & \text{if} \quad r_i \leq 0 \\ 0, & \text{if} \quad r_i > 0 \end{cases} \tag{2}$$

$$S_{\text{downside}} = 2 \times E\left\{\sum [r - E(r)]^2\right\} \tag{3}$$

Table 1 Uncertainty categorization

Development uncertainty	Operational uncertainty
Political uncertainty: uncertainty of development funding instability	Political uncertainty: uncertainty of operational funding instability
Requirements uncertainty: uncertainty of requirements stability	Lifetime uncertainty: uncertainty of performing to requirements in a given lifetime
Development cost uncertainty: uncertainty of developing within a given budget	Obsolescence uncertainty: uncertainty of performing to evolving expectation in a given lifetime
Development schedule uncertainty: uncertainty of developing within a given schedule profile	Integration uncertainty: uncertainty of operating within other necessary systems
Development technology uncertainty: uncertainty of technology to provide performance benefits	Operations cost uncertainty: uncertainty of meeting operations cost targets
	Market uncertainty: uncertainty in meeting demands of an unknown market
Model uncertainty	

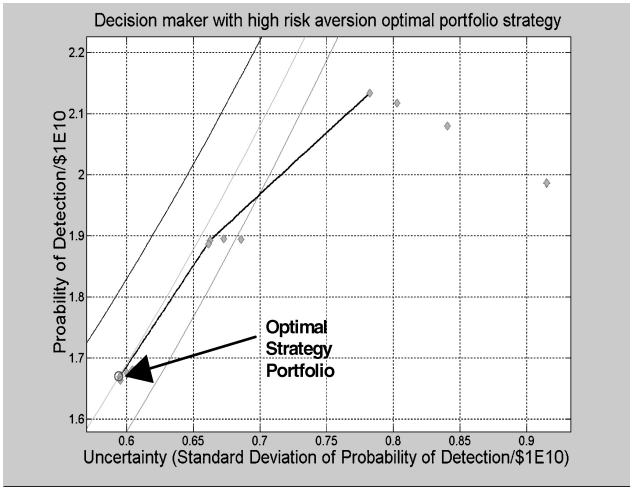

Fig. 3 Optimal investment strategy for high-risk aversion decision maker.

Table 2 Composition of TechSat 21 decision maker strategies

Decision maker type	Percentage of portfolio, %	Architecture design vector {altitude, satellites per cluster, number of clusters, number of planes, antenna power, antenna diameter}	Total utility/$	σ
High-risk aversion	100	{800, 4, 42, 6, 1000, 2.5}	1.67	0.59
		Portfolio value and uncertainty	1.67	0.59
Moderate-risk aversion	100	{800, 4, 42, 6, 900, 3}	1.89	0.66
		Portfolio value and uncertainty	1.89	0.66
Low-risk aversion	100	{800, 4, 42, 6, 900, 3.5}	2.13	0.78
		Portfolio value and uncertainty	2.13	0.78

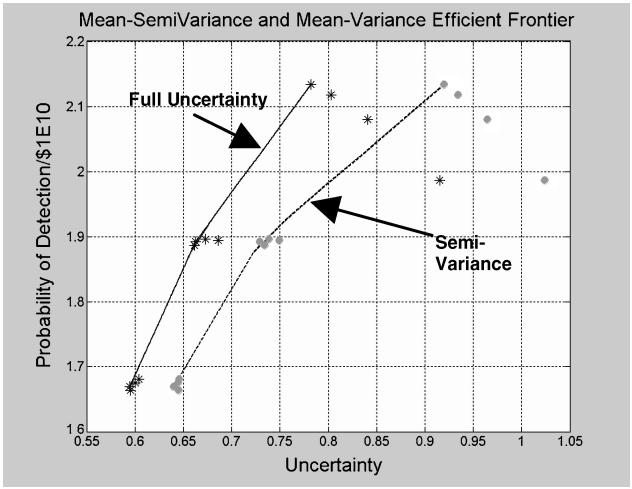

Fig. 4 TechSat 21 portfolio analysis with full uncertainty and semivariance.

thus creating a downside covariance matrix as

$$Q_{\text{downside}} = \begin{bmatrix} S_{d1}^2 & \rho_{2,1}S_{d2}S_{d1} & \rho_{3,1}S_{d3}S_{d1} & \bullet & \rho_{n,1}S_{dn}S_{d1} \\ \rho_{1,2}S_{d1}S_{d2} & S_{d2}^2 & \rho_{3,1}S_{d3}S_{d1} & \bullet & \rho_{n,2}S_{dn}S_{d2} \\ \rho_{1,3}S_{d1}S_{d3} & \rho_{2,3}S_{d2}S_{d3} & S_{d3}^2 & \bullet & \rho_{n,3}S_{dn}S_{d3} \\ \bullet & \bullet & \bullet & \bullet & \bullet \\ \rho_{1,n}S_{d1}S_{dn} & \rho_{2,n}S_{d2}S_{dn} & \rho_{3,n}S_{d3}S_{dn} & \bullet & S_{dn}^2 \end{bmatrix} \tag{4}$$

Finally, the portfolio algorithm is implemented in the similar manner to traditional portfolio theory, only substituting Q_{downside} for Q, as shown in Eq. (1) to define an efficient frontier based on semivariance. The efficient frontier for both full uncertainty portfolio analysis and semivariance analysis is shown in Fig. 4, which illustrates the there is more risk in the tradespace than would be perceived if uncertainty were used as a surrogate for risk.

Under the efficient frontier using semivariance, the high-risk averse decision maker's portfolio strategy would remain the same because there are no less uncertain architectures to pursue. The moderate decision maker has shifted to the same single asset portfolio strategy as the high-risk aversion decision maker given the increased risk, whereas the low-risk averse decision maker had no change to the portfolio because the increased uncertainty was not enough to move the optimum portfolio.

Observations from TechSat 21

The level of uncertainty in the tradespace was considerable; nevertheless, the optimal portfolio strategies for three decision makers comprised single architectures. Of the architectures evaluated, there was not enough independence with respect to uncertainty for diversification. In the next two cases, diversification does influence the optimal strategy.

The inclusion of the framework did illustrate the large amount of uncertainty associated with each architecture in the tradespace, thus, allowing the decision maker to base decisions to see the risk behind the otherwise deterministic assumptions. The uncertainty analysis further illustrated the ability to compare architectures in the tradespace, understand the relative sensitivities, and trace those sensitivities back to sources of uncertainty. This traceability allows designers to concentrate on either modeling with more resolution or building in enough margins in their designs to accommodate the resultant possibilities.

Broadband Mission and Model Description

This commercial mission allows for uncertainty analysis in a context of market uncertainty. Numerous examples of the effects of market uncertainty can be seen in the space industry, ranging from uncertainties of launch vehicle capacity to meet evolving needs to market uncertainties that have defined the bankruptcies of Iridium and GlobalStar. Whereas a space system has been chosen to service this market, the details of the architecture have not been defined and instead have been left open for defining the tradespace. Six tradable parameters define the boundaries of the tradespace: 1) altitude, 2) inclination, 3) number of satellites per plane, 4) number of planes, 5) payload power, and 6) antenna area.

GINA Model

The model, based on work by Kashitani,[4] initiates with the definition of a constants vector containing parameters of the design that remain constant across all of the architectures being evaluated. Examples of the constants include market size and distribution, satellite sizing ratios, and launch vehicle performance.

The simulation is relatively course in system design detail, but serves as a good case for analysis because of the market models that exemplify circumstances where market uncertainty can have the driving effects on outcomes. The flow of the model begins with a relative sizing of the spacecraft based on rules of thumb and the design vector inputs. For example, from the antenna power and antenna size, the relative mass and size of the spacecraft can be determined from sizing relationships commonly used in conceptual design.[5] After the relative size of the spacecraft is calculated, Satellite Tool Kit® is used to propagate the satellites in their individual orbits and capture ephemeris that can be used in the coverage model. The coverage model calculates a global map of acceptable coverage that is achieved from the space segment of the architecture, based on probabilities of satellites in view. The system capacity model then generates the total subscribers that the architecture being evaluated could support. The capacity of the architecture and its coverage are then compared with a market demand model that defines the number of likely subscribers over the course of a given year. The launch module then creates a launching scheme based on the orbital characteristics, as well as mass and size characteristics of the satellite constellation. The system component costs are then calculated, as well as the total system cost that is then transformed to present valuation. The final module accepts the inputs from the previous models and generates a number of outcome measures, that is, profit, cost per billable hour, etc.[4]

Model Results

With use of a heuristic search of the design tradespace,[2,4] 13 Pareto optimal architectures were found. The calculated results are the expected outcomes for the 13 architectures on the Pareto front, but of course there is uncertainty that surrounds each expectation. From this tradespace of total subscriber hours generated by the space system and the system cost, a billable hour per dollar-invested metric (subscriber hour/$) is developed that is used later as the single measure of value for the decision maker.

Uncertainty Quantification

Once the initial sources of uncertainty were identified and quantified, a Monte Carlo uncertainty propagation technique was used to develop the embedded uncertainty for each architecture. Because the broadband GINA model is relatively coarse, a good deal of the uncertainty being quantified arises from the rules of thumb being used in the model. However, because of the commercial nature of the case, market uncertainties are also introduced.

The cost module for this system used cost-estimating relationships (CER) to transform mass into cost for development of the spacecraft. These CERs served as one source of cost uncertainty. For example, the historical rule of thumb for theoretical first unit cost per kilogram is $84,000. A normal distribution centered on $84,000 with a standard deviation of $10,000 was used in the simulation models to capture the expectation and uncertainty associated with the cost estimating relationship.

The market uncertainty in this case is arising from the estimation of three main parameters: 1) total market size of broadband

customers, 2) percent market capture for this project, and 3) discount rate used in the cash flow analysis. These three sources of market uncertainty serve as representative examples of market uncertainty. Others could have been included, such as uncertainty in market geographic distribution or competition scenarios. Kelic investigated a number of market uncertainties that include those just listed in her analysis of potential space-based broadband delivery systems.[6] Uncertainty in total market size is modeled using a lognormal distribution that is consistent with pervious market analysis of the broadband market potential. The percent market capture is another source of uncertainty. Even with a precise market, there is no way to know what competitors you will have and what customers will prefer. Again a lognormal distribution is used here to represent an expected market capture of 7.5% and the distribution around that.

Finally, a discount rate was used in some of the calculations to generate net present values for various architecture outcomes. The discount rate uncertainty was represented by a normal distribution with mean of 30% with a standard deviation of 7.5%. Although market uncertainties exist in the broadband case, by no means are market uncertainties isolated to commercial ventures. Military and civil systems also suffer from market uncertainties in a number of ways, ranging from competition to demand for the system, to unknown responses from adversaries.

Because the simulation model was relatively course, there were a number of design rules of thumb used to size features of the architectures, including payload power per unit mass, mass fraction of the payload with respect to dry mass, fraction of dry mass in wet mass, and density of satellite. These rules of thumb are based on historical trends, and most have associated with them an expected scaling factor and a standard error.[7] These model uncertainties were incorporated into the analysis.

To calculate the embedded uncertainty in each architecture, the set of individual sources of uncertainty is built into the constants vector. The first step is to sample the constants vector under conditions of uncertainty, and results are captured for each architecture. Next, a new constants vector is selected from the distribution of possible constants vectors, and the simulation is run again. This process of selecting a constants vector is repeated until a populated distribution of outcome measures is generated.

The end result of the uncertainty propagation is an ordered set of outcomes for every architecture considered. These data can be used to create statistical measures of uncertainty for a single architecture and also to generate pairwise correlation coefficients necessary in portfolio optimization. Figure 5 shows a snapshot of the embedded uncertainty that was calculated for each architecture on the Pareto optimal front. The diamonds represent the expected value of the architecture in terms of system cost and total subscriber hours, whereas the ellipses represent the uncertainty of each architecture in both dimensions.

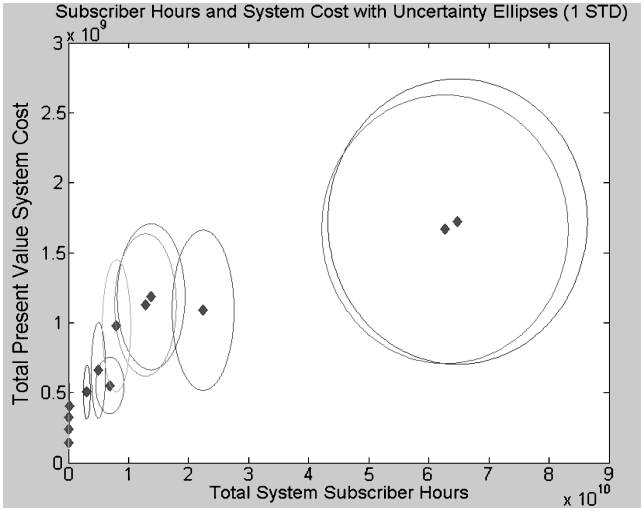

Fig. 5 Broadband tradespace with the inclusion of uncertainty.

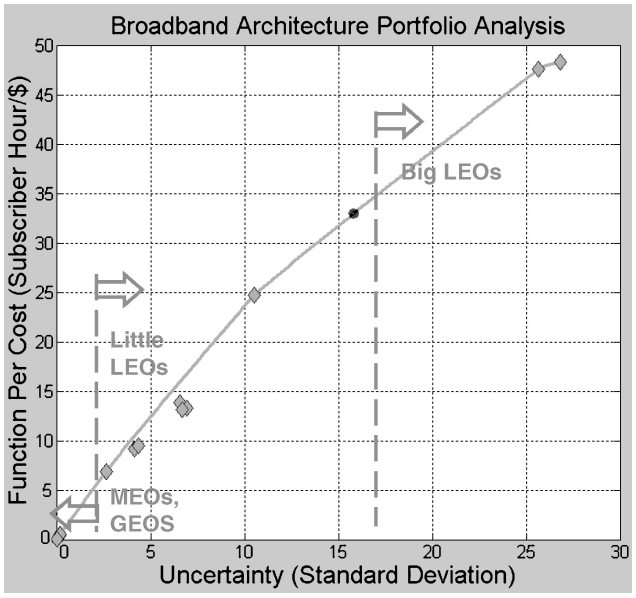

Fig. 6 Broadband efficient frontier.

Portfolio Analysis

Portfolio analysis provides a context in which tradeoffs of uncertainty and value, subscriber h/$, can be made. With use of an expected return and covariance matrix based on 100 observations of 13 architectures, the portfolio optimization algorithm was applied to generate the efficient frontier. An immediate observation from the portfolio tradespace, as shown in Fig. 6, is the clear demarcation of geosynchronous-Earth-orbit (GEO), medium-Earth-orbit (MEO), and low-Earth-orbit (LEO) architectures along measures of value and uncertainty.

Quantifying Decision Maker Risk Aversion

Three decision makers were chosen with risk aversion coefficients k of 0.03, 0.1, and 1 to illustrate different optimum portfolios. The first decision maker was highly risk averse, $k = 1$, and found optimum strategy in the lower-left-hand corner of the efficient frontier. The composition of the strategy is defined in Table 3. There were lower risk assets for which the decision maker could have invested, such as the one GEO architecture on the Pareto optimal front, but this decision maker desired more return that the lower risk architectures could provide.

The second decision maker investigated has a k value equal to 0.1. In most cases, this value would not be considered a moderate level of risk aversion, but the phrase is used here to show the relative preference to uncertainty of three decision makers. The composition of this portfolio lies at a single architecture, a LEO architecture consisting of 40 satellite constellation each with a 2-m^2 antenna and 1-kW power.

The third decision maker has a very low level of risk aversion, $k = 0.03$, and the optimal strategy resides in the upper-right corner of the efficient frontier. The reason for large LEO architectures dominating this portfolio is the larger the constellation of satellites is, the greater capacity the system has to achieve subscriber hours if the market conditions are good. However, under adverse market conditions, the system will not achieve the subscribers expected, and it will have required a significant capital investment to construct it.

Implications of Incorporating the Extensions to Portfolio Theory

The classical implementation of portfolio theory has been presented using uncertainty as a surrogate for risk, but, in fact, the two can be separated, as shown earlier. Furthermore, the low-risk aversion decision maker has a suggested optimal portfolio that consists of more than one asset. What is the extra cost of that portfolio and how should a cost benefit trade be made? To find the answer, the correlation coefficient of the portfolio members is used as a starting point.

Table 3 Composition of broadband high-risk aversion decision maker strategy

Decision maker type	% of portfolio	Architecture design vector {altitude, inclination, satellites per plane, planes, power, antenna area}	Subscriber h/$	σ
High-risk aversion	55	{MEO, 0, 8, 1, 1, 3}	0.5	0.2
	45	{LEO, 0, 7, 1, 2, 0.5}	6.9	2.7
		Portfolio value and uncertainty	3.4	1.3
Moderate-risk aversion	100	{LEO, 45, 5, 8, 1, 2}	24.7	10.5
		Portfolio value and uncertainty	24.7	10.5
Low-risk aversion	9	{LEO, 45, 5, 8, 1, 2}	24.7	10.5
	2	{LEO, 45, 7, 10, 1, 3}	48.3	26.8
	89	{LEO, 60, 6, 10, 1, 3.5}	47.6	25.6
		Portfolio value and uncertainty	45.5	24.2

Differentiating risk from uncertainty. When the algorithm in Eq. (1) and Q_{downside} from Eq. (4) are used an efficient frontier for semivariance can be calculated in the same manner performed earlier in the case. The results show there is less risk in the tradespace than would be perceived if uncertainty were used as a surrogate for risk. Using the same decision makers used earlier, we see some shifts in the three decision makers' optimum portfolios. The highly risk averse decision maker has not changed strategy nor has the moderate-risk aversion decision maker, despite the lower perceived risk in the tradespace under the semivariance calculation. However, the low-risk averse decision maker has seen a shift in strategy. The earlier portfolio of three assets has become a portfolio of two, namely, the architectures that had the highest values.

Cost of diversification. Some of the optimal portfolio strategies that have been found in this case have included more than one asset and, therefore, more than one architecture to pursue in design. To calculate the cost to diversify into a portfolio, the individual assets should be closely looked at by the designers and decision makers. For example, two LEO architectures with 45-deg inclination operating at 1 kW and 2-m^2 antennas and having only a small difference in the number of satellites in slightly different planes will probably not incur twice the design cost of a single architecture because of the commonality between the two architectures. In contrast, a two-asset portfolio with a large LEO architecture requiring many ground stations and a two-satellite GEO architecture might represent a significantly higher cost to develop than either of the two individually.

A relative measure of the cost of diversification is used to judge the extra cost of carrying a portfolio based on the correlation of assets in the portfolio, as proposed by Walton.[8] For example, the low-risk aversion decision maker under the full uncertainty distribution would have a cost to diversify equal to 0.5% of the cost to design the architecture with the design vector {LEO, 45, 5, 8, 1, 2} plus 0.1% of the cost to design the architecture with the design vector {LEO, 45, 7, 10, 1, 3}. Therefore, the total cost to proceed with the portfolio would be the cost of designing the majority constituent in the three-architecture portfolio plus this additional cost to diversify. This type of calculation can provide the basis for additional consideration by the decision maker on whether or not to proceed with the portfolio strategy. The actual cost to diversify will be case specific and should be looked at carefully by the designers and decision makers.

Observations from Broadband Case Study

This case demonstrated the applicability of the uncertainty analysis approach to space-based broadband communications architecture. Market and model uncertainty were explored as primary sources of uncertainty, and the case demonstrated how significant these sources could be to the overall value of a given architecture. The role of downside semivariance focus was also demonstrated, in contrast to a full uncertainty.

The intuitive observations that comes from the analysis such as LEO architectures having predominantly greater uncertainty than MEO and GEO architectures is reinforcing to current speculations, but the case provides a quantitative base for exploring the intuition in more detail. Moreover, an interesting note on this case is how real-world systems are acting with respect to the efficient frontier that was developed. The Teledesic Space System has been in development for some time. Initially conceived as a very large, LEO constellation of satellites, the system would provide global broadband capability with very low latency and at a reasonable price. The original concept was released in 1994 as having 840 satellites at development cost of $6.3 billion and total life-cycle cost of $17.8 billion.

In 1998, Teledesic went through a dramatic redesign from 840 satellites in LEO to 288 satellites. As was shown in the analysis, this shift to fewer spacecraft lowered the potential market capture of the system, but also lowered the exposure to risk that the system would have from the upfront development cost investment. In February 2002, a Teledesic architecture redesign was publicly released consisting of 12 satellites in MEO at a development cost of $1 billion with 18 more MEO satellites deployed at a later date to supplement coverage to achieve global capacity. Again, this change in architecture is a downward movement on the efficient frontier, opting for less capacity and subscriber hours/$, but at a significantly lower cost than the LEO systems.

Terrestrial Observer Swarm Mission and Model Description

The first iteration A of terrestrial observing swarms (A-TOS) mission has the primary objective of collecting and disseminating fine measurements of the ionosphere. The science customer would use the data as inputs to a ionospheric behavior simulation model. An understanding of the ionosphere's composition at fine detail would allow for more accurate prediction and mitigation of errors in communication and location measurement. Potential tactical benefits of a detailed mapping of the ionosphere begin to paint a clear picture of the potential value of such a mission beyond the pure science of ionospheric mapping.

A-TOS Mission

The overarching goal of the A-TOS project was to design a space system that captured both the large-scale and timescale aspects of the ionosphere, as well as the detailed, small timescale fluctuations that are less predictable. One of the most interesting features of the A-TOS model developed was the use of utility measures to define goodness in the tradespace of architectures. Instead of using a set of performance measures, such as usable bytes delivered or resolution and accuracy, a nontraditional approach, utility theory,[9] was applied to the problem of balancing the many sets of customer preferences that were involved in the program.

Utility theory allows the designer to capture preferences of the customer in mathematical equations that provide for customer-in-the-loop tradeoffs, although not necessarily requiring their physical presence. The high-level concept employed to carry out the A-TOS mission was clusters of satellites taking direct measurement of ionospheric conditions as the individual satellites passed through it. The payload would be a passive payload consisting primarily of planar langmuir probes to record charged-particles densities. This approach has the benefits of having a relatively simple passive payload that

requires little power, mass, and records data that need little postprocessing to arrive at useful information for the customer.

Derived Utility Function and System Analysis Model

The utility of the A-TOS system was derived from an architecture's ability to satisfy three distinct sub-missions. The first, the low-latitude survey mission, was an equatorial region survey that would identify unstable regions of the ionosphere near the equator. The second mission, the low-latitude snapshot mission, would require the space system to initiate an extensive data collection of an unstable region once the first mission identified an instability. The third mission was to perform a high-latitude survey that would accurately measure relative ionospheric density correlated with global positioning system-to-ground data.

The low-latitude survey mission was to measure the low-latitude characteristics of the ionosphere at a sampling rate of approximately 1 Hz. From this information, the customer's model could be populated with the large-scale characteristics of the ionosphere. The low-latitude snapshot submission would be important once the survey mission identified a ionosphere disturbance. With use of a swarm of satellites, fine-scale measurements of the anomaly would be collected. The last submission is a high-latitude survey. The major charged-particle concentration in the ionosphere is centered about the equatorial band and the high-latitude region. Although not as significant a submission as the low-latitude missions, the high-latitude mission would provide further population of the science community's global ionospheric model and prediction ability.

From the described missions, utility functions were calculated for each of the missions, as a function of each mission's attributes, as notionally shown in the following equations. For example, the low-latitude survey mission was a function of individual sample observations and the location and time of day of each measurement. Thus,

$$U_{\text{low\_surv}} = f(X_1, X_2, \ldots, X_m) \tag{5}$$

$$U_{\text{low\_snap}} = g(Y_1, Y_2, \ldots, Y_m) \tag{6}$$

$$U_{\text{high\_surv}} = h(Z_1, Z_2, \ldots, Z_n) \tag{7}$$

Additionally, a total architecture utility variable was defined as a weighted sum of the two separate mission utilities, as shown in Eq. (8). Although this equation is a simple linear aggregation of the multiple elements of utility, it provided a first look at how ideas of utility could be incorporated into the space systems conceptual design process. Considerable progress has been made on subsequent design iterations that exploit the full potential of multi-attribute utility theory:

$$U_{\text{total}} = U_{\text{high\_surv}}/U_{\text{max high\_surv}} + 2^*(U_{\text{low\_surv}} + U_{\text{low\_snap}})/(U_{\text{low\_surv}} + U_{\text{low\_snap}})_{\max} \tag{8}$$

The design vector consisted mainly of orbital parameters because the mission was driven by the in situ locations of individual satellites throughout the mission lifetime, including 1) altitude, 2) subplanes per swarm, 3) satellites per swarm, 4) suborbits per swarm, 5) subplane yaw, and 6) separation distance. The simulation models developed during the A-TOS design effort were based on heritage models developed under the GINA method[1] but went further to apply utility theory to capture the preferences of the customer in the simulation. A utility function was formulated, as described earlier, and incorporated into the system simulation to generate outcome measures that would enable informed tradeoffs of potential architectures.

Model Results

Over 4000 architectures were evaluated using the simulation model. After calculating the expected outcomes for these potential architectures, the tradespace was explored along the utility and cost measures developed in the early problem formulation. Figure 7 shows how the tradespace took shape in terms of low-latitude utility, high-latitude utility, and cost. Each shaded square in the chart

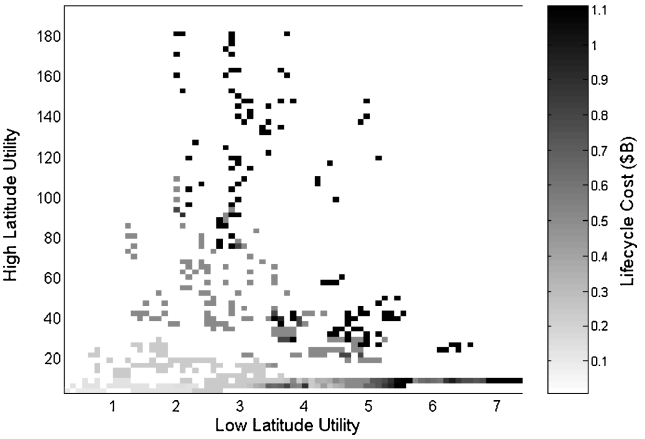

Fig. 7 Low- and high-utility tradespace vs life-cycle cost.

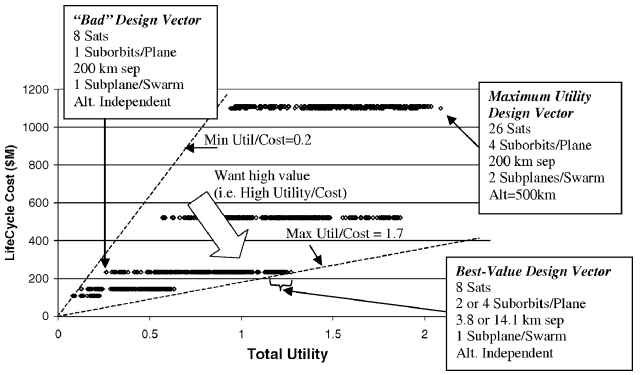

Fig. 8 A-TOS cost and utility tradespace.

represents at least one specific architecture concept, as defined by a unique design vector. The first conclusion that can be drawn from this tradespace is that utility increases with increasing cost. It is further evident though that there are some relatively inexpensive architectures that accomplish the low-latitude mission quite well, but do not perform very well in the high-latitude mission.

When the tradespace is explored further, the individual points can be identified by what architecture they represent, as well as what characteristics drive the performance outcomes. Figure 8 shows the total utility, from Eq. (8), and cost predicted outcomes for 1380 architectures, which are represented as diamonds in the plot. We have limited the uncertainty analysis to the Pareto optimal front of architectures in the tradespace, plus 24 additional near Pareto optimal architectures, primarily for computational efficiency.

Uncertainty Quantification

The major technical uncertainty that was included came from the mean time to failure (MTTF) for a single satellite in the constellation. Because the MTTF is a representative reliability of the entire satellite, it is a very difficult number to measure. Small satellites such as those presented have previously used 500 months as the MTTF. However, there are not a lot of these distributed satellite systems in operation, and so the reliability warranted the inclusion of uncertainty bounds. A normal distribution with a standard deviation of 50 months was used to represent the uncertainty in MTTF.

The cost uncertainty arose from both cost to develop and the cost of operations. The uncertainty in the cost of development of the satellite bus was captured using the standard error in the historical cost estimating relationships used in the simulation models. The development cost uncertainty for the payload was also included. The operations cost uncertainty arose from uncertainty in the estimation of the individual sources that contribute, such as the number of engineers and operators required for maintaining the system and the uncertainty in the cost of ground software and equipment.

Because this case relied on utility as the key decision criteria, an element of utility uncertainty was included in the analysis. The

Table 4 Composition of A-TOS decision maker strategy

Decision maker type	% of portfolio	Architecture design vector {satellites per swarm, suborbits, size, yaw, subplane, altitude}	Total utility/$	σ
High-risk aversion	52	{26, 4, 14.1, 60, 2, 700}	2.4	0.9
	48	{2, 1, 3.8, 30, 1, 300}	1.9	0.8
		Portfolio value and uncertainty	2.2	0.7
Moderate-risk aversion	57	{26, 4, 14.1, 60, 2, 700}	2.4	0.9
	28	{4, 2, 3.8, 30, 1, 500}	4.2	1.7
	15	{4, 1, 14.1, 0, 1, 700}	4.1	1.6
		Portfolio value and uncertainty	3.2	1.1
Low-risk aversion	83	{8, 4, 14.1, 30, 1, 700}	5.4	2.3
	17	{4, 2, 3.8, 30, 1, 500}	4.2	1.7
		Portfolio value and uncertainty	5.2	2.2

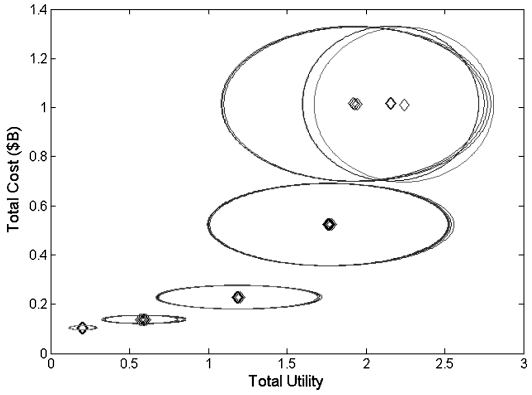

Fig. 9 A-TOS utility and cost tradespace with uncertainty ellipses (one standard deviation).

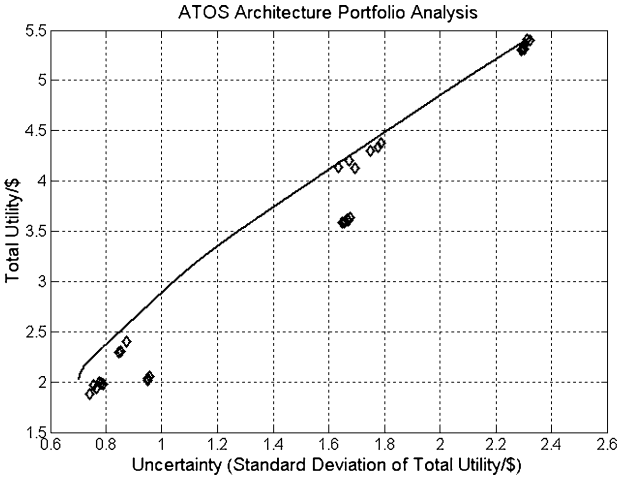

Fig. 10 Efficient frontier in the A-TOS tradespace.

combined low-latitude mission and high-latitude mission were difficult for the customer to distinguish in terms of precise relative value, so that a nominal value of 2:1 was used as the utility ratio of the combined low-utility mission to the high-utility mission, as was shown in Eq. (8). Instead of using this ratio, the relative worth of the high-latitude mission over the low-latitude mission was modeled as a probabilistic density function with a mean of 2 and a standard deviation of 1.

The model uncertainty in the A-TOS case study arose from the designers' inability to quantify precisely different aspects of the system through mathematical formulation. Instead, design rules of thumb or parametric relationships are used that are based on historical observations. Two model uncertainties in the case of A-TOS were the satellite density, which is used to calculate the derived mass and overall structure within the model, and the learning curve used to estimate production costs for more than one satellite.

Once the sources of uncertainty have been identified and each has been quantified and inserted into the constants vector, a Monte Carlo sampling routine, as already described, was conducted with the goal of developing distributions of outcomes for each of the architectures evaluated. Figure 9 presents a snapshot of the embedded uncertainty that was calculated for each architecture on the Pareto optimal front. The points represent the expected value of the architecture in terms of cost and total utility, whereas the ellipses represent the uncertainty of each architecture in both dimensions.

Portfolio theory abstracts uncertainty characteristics to simple measures of expectation and variance that are consistent with Gaussian distribution. The individual architecture uncertainty distributions should be investigated to satisfy this assumption that the characteristics of the uncertainty distribution can indeed be captured by these simple measures. Normality can be tested using statistical measures such as skewness and kurtosis as well as graphical techniques. When the Shapiro–Wilk test for normality, is used the hypothesis for normality, is used, could not be rejected for any of the architectural distributions created in the A-TOS systems analysis.

Portfolio Analysis

With an expected return and covariance matrix based on 60 observations of 30 architectures used, the portfolio optimization algorithm was applied to generate the efficient frontier. Figure 10 shows the efficient frontier, as derived under the classic portfolio optimization algorithm in Eq. (1). The efficient frontier extends beyond the performance achieved by any single architecture and is an important finding because it shows that portfolios can provide more benefit to the decision maker than would otherwise be possible with a single asset. The reason for the extension beyond any single architecture can be traced back to Fig. 7. Some architectures achieve a very high level of low-latitude value at low cost but perform the high-latitude mission poorly, whereas others perform well in both low- and high-latitude missions. Because of these two different approaches to achieving total value, there arises a chance to diversify uncertainty. The uncertainty diversified is not enormous, but it is measurable and presents one of the first illustrations that portfolio assessment in space systems can help decision makers achieve higher returns for a given level of uncertainty than they otherwise could with single assets.

Quantifying Decision Maker Risk Aversion

By the use of three representative decision makers, the overall sensitivities of the portfolio can be observed and outcomes compared to demonstrate the adaptability of the uncertainty analysis approach to a large range of decision makers who become involved in the development of space systems. The first decision maker has a relatively high-risk aversion coefficient $k = 2$. The composition of the optimum portfolio for this decision maker is 48% of one architecture and 52% of another, as shown in Table 4. The two architectures that have been selected behave differently enough to move the curve beyond a simple linear combination of the two and provide measurable value through diversification. A strategy has been created that has less uncertainty than either of the portfolio assets. The

Table 5 Composition of A-TOS high-risk aversion decision maker strategy using semivariance

Decision maker type	% of portfolio	Architecture design vector {satellites per swarm, suborbits, size, yaw, subplanes, altitude}	Total utility/$	σ
High-risk aversion	64	{26, 4, 14.1, 60, 2, 700}	2.4	0.8
	36	{2, 1, 3.8, 30, 1, 300}	2.0	0.8
		Portfolio value and uncertainty	2.3	0.7
Moderate-risk aversion	65	{26, 4, 14.1, 60, 2, 700}	2.4	0.8
	35	{4, 2, 3.8, 30, 1, 500}	4.3	1.8
		Portfolio value and uncertainty	3.1	1.0
Low-risk aversion	100	{8, 4, 14.1, 30, 1, 700}	5.4	2.3
		Portfolio value and uncertainty	5.4	2.3

majority of the portfolio is occupied by the architecture that was identified as having the maximum utility in the tradespace in Fig. 8, whereas the remaining portfolio includes a much smaller architecture of only 2 satellites, compared to 26, and has a much smaller cost. The two combine synergistically in this portfolio because the two architectures are achieving total utility per dollar in two ways. The 26 satellites architectures is achieving both the low- and high-latitude missions but at a high price. The two-satellite mission is achieving good results on the low-latitude survey submission, but does not have enough satellites to do a good job at either the low-latitude snapshot mission or the high-latitude survey. On the other hand, the two-satellite architecture is inexpensive; thus, it achieves a good total utility per dollar.

The next decision maker presented has a more moderate-risk aversion coefficient $k = 1$. Without the creation of a portfolio, the decision maker would have to settle for single assets that meet the risk aversion criteria but achieve much lower total utility per dollar, or the decision maker would need to accept a higher level of risk than the aversion coefficient would predict to be comfortable to achieve a high level of total cost per dollar. The ability of portfolio theory to create continuous investment strategies is another benefit that can not be achieved with single assets.

The final decision maker has a relatively low-risk aversion coefficient $k = 0.4$. With a relatively low level of risk aversion, this type of decision maker is trying to get the most value out of the system with relatively little worry about the risk that the solution might carry. Notice one architecture from the moderate-risk averse decision maker is kept, but a new architecture has been added as well. This architecture was called out in Fig. 8 as the best value design. Indeed, this architecture did have the highest total utility per dollar, but it also had the highest level of uncertainty for any of the architectures.

Implications of Incorporating the Extensions to Portfolio Theory

Although classic portfolio techniques were used, the two extensions to portfolio theory illustrated earlier could also be applied to glean new information. The first extension is separating the risk from the uncertainty and is useful to illustrate that architectures are more or less risky than their uncertainty distributions might lead to one to believe. The second extension is to quantify the cost of carrying a portfolio of architectures, rather than any single asset.

Differentiating risk from uncertainty. When the algorithm in Eq. (1) and Q_{downside} from Eq. (4) were used, the semivariance scaled efficient frontier was found, with the key takeaway being the risk to a given decision maker was overestimated using the full variance as a measure of risk. The first decision maker was the high-risk aversion decision maker. Under the efficient frontier using semivariance, the optimal portfolio strategy has changed only in percentage investment in each of the assets in the portfolio, as shown in Table 5. The optimal portfolio now has a higher degree of emphasis on the higher return asset. The moderate-risk decision maker has kept two of the previous three-asset portfolio. The low-risk aversion decision maker has moved his optimal strategy to a one-asset portfolio.

Cost of diversification. A measure of the cost of diversification can be used to judge the relative extra cost of carrying a portfolio based on the correlation of assets in the portfolio. For example, the high-risk aversion decision maker under the full uncertainty distribution would have a cost to diversify equal to 33% of the cost to design the two-satellite architecture. This high cost to diversify is based on the low correlation that exists between the two assets, 0.598. In contrast, the cost to diversify of the low-risk averse decision maker would be only 3.5% of the cost to design the four-satellite architecture in the portfolio. This lower additional cost is due to the higher degree of correlation that exists, 0.965.

Observations from A-TOS Case Study

This case provided an opportunity to implement the uncertainty analysis approach in the context of a scientific space system. The A-TOS case study demonstrated the use of the uncertainty analysis method in a system exploration that centered around utility per dollar as a fundamental decision criteria. The approach captures the benefits that portfolio analysis can provide to a decision maker by creating investment strategies for design that achieve higher value for lower uncertainty than would be possible with any single asset, as illustrated by the high-risk averse decision maker whose optimal portfolio consisted of architectures that achieved value through different approaches and, therefore, reacted differently to uncertainty.

Conclusions

This paper presented portfolio theory and optimization as one approach to manage uncertainty in the conceptual design of space systems. There are a number of benefits that come from using this approach over previous techniques of dealing with uncertainty in the conceptual design. First and foremost, portfolio theory can provide strategies of investment that can be tailored to a decision maker's risk aversion and in some cases provide higher return and lower uncertainty than would otherwise be obtained. Second, continuous investment opportunities are created for decision makers along the efficient frontier. Beyond these two benefits, portfolio theory provides for the quantification of diversity in the tradespace through the covariance matrix and also illustrates the importance of separating the downside of uncertainty from total uncertainty in making decisions.

Acknowledgments

The authors gratefully acknowledge the financial support for this research from the Space Systems Policy and Architecture Research Consortium, a joint research program funded by the U.S. government involving the Massachusetts Institute of Technology, the California Institute of Technology, and Stanford University. The authors thank Edward Crawley, Earll Murman, Joyce Warmkessel, Hugh McManus, Cyrus Jilla, and Annalisa Weigel (all of the Massachusetts Institute of Technology) for their insights and feedback on this research work. William Borer, Willam Kaliardos, David Ferris, Andre Girard, Adam Ross, Daniel P. Thunnisen, and Brandon Wood produced much of the terrestrial observer system A simulation models.

References

[1]Shaw, G., Miller, D., and Hastings D., "Development of the Quantitative Generalized Information Network Analysis (GINA) Methodology for

Satellite Systems," *Journal of Spacecraft and Rockets*, Vol. 38, No. 2, 2001, pp. 257–269.

[2]Jilla, C., "Multidisciplinary Design Optimization Methodology for the Conceptual Design of Distributed Satellite Systems," Ph.D. Dissertation, Dept. of Aeronautics and Astronautics, Massachusetts Inst. of Technology, Cambridge, MA, June 2002.

[3]Shaw, G. B., "The Generalized Information Network Analysis Methodology for Distributed Satellite Systems," Sc.D. Dissertation, Dept. of Aeronautics and Astronautics, Massachusetts Inst. of Technology, Cambridge, MA, Feb. 1999.

[4]Kashitani, T., "Development and Application of an Analysis Methodology for Satellite Broadband Network Architectures," AIAA Paper 2002-1417, May 2002.

[5]Reeves, E., "Spacecraft Design and Sizing," *Space Mission Analysis and Design*, 2nd ed., Microcosm, Torrance, CA, 1992, pp. 285–337.

[6]Kelic, A., "Assessing the Technical and Financial Viability of Broadband Satellite Systems Using a Cost per T1 Minute Metric," M.S. Thesis, Dept. of Aeronautics and Astronautics, Massachusetts Inst. of Technology, Cambridge, MA, May 1998.

[7]Wong, R., "Cost Modeling," *Space Mission Analysis and Design*, 2nd ed., Microcosm, Torrance, CA, 1992, pp. 715–740.

[8]Walton, M., "Managing Uncertainty in Space Systems Conceptual Design Using Portfolio Theory," Ph.D. Dissertation, Dept. of Aeronautics and Astronautics, Massachusetts Inst. of Technology, Cambridge, MA, June 2002.

[9]Von Neumann, J., and Morgenstern, O., *Theory of Games and Economic Behavior*, 3rd ed., Princeton Univ. Press, Princeton, NJ, 1953, pp. 15–29.

J. Korte
Guest Editor